Flexibility and Bioactivity of Insulin: an NMR Investigation of the Solution Structure and Folding of an Unusually Flexible Human Insulin Mutant with Increased Biological Activity[†,‡]

Danielle Keller,[§] Rikke Clausen,[||] Knud Josefsen,[||] and Jens J. Led*[,§]

Department of Chemistry, University of Copenhagen, The H. C. Ørsted Institute, Universitetsparken 5, DK-2100 Copenhagen Ø, Denmark, and The Bartholin Institute, Kommunehospitalet, DK-1399 Copenhagen K, Denmark

Received April 20, 2001; Revised Manuscript Received June 18, 2001

ABSTRACT: The structure and folding of a novel human insulin mutant, [Thr(B27) → Pro, Pro(B28) → Thr]insulin (PT insulin), in aqueous solution and in mixtures of water and 2,2,2-trifluoroethanol (TFE) have been studied by NMR spectroscopy. It was found that PT insulin has a highly flexible structure in pure water and is present in at least two different conformations, although with an overall tertiary structure similar to that of native insulin. Furthermore, the native helical structures are poorly defined. Surprisingly, the mutant has a biological activity about 50% higher than native insulin. In contrast, in TFE/water solution the mutant reveals a propensity of forming a well-defined structure at the secondary structure level, similar to monomeric native insulin. Thus, as shown by a detailed determination of the structure from 208 distance restraints and 52 torsion angle restraints by distance geometry, simulated annealing, and restrained energy minimization, the native insulin helices (A2−A7, A13−A19, and B10−B19) as well as the β-turn (B20−B23) are formed in 35% TFE. However, the amount of tertiary structure is decreased significantly in TFE/water solution. The obtained results suggest that only an overall tertiary fold, as observed for PT insulin in pure water, is necessary for expressing the biological activity of insulin, as long as the molecule is flexible and retains the *propensity* to form the secondary structure required for its receptor binding. In contrast, a compact secondary structure, as found for native insulin in solution, is unnecessary for the biological activity. A model for the receptor binding of insulin is suggested that relates the increased bioactivity to the enhanced flexibility of the mutant.

The structural basis of the function of insulin has been a subject of intense investigation in recent years. The structures of numerous insulin mutants have been solved and their in vivo activities have been compared in order to elucidate the correlation between the structure and function of insulin. However, the structure of the hormone bound to the insulin receptor (IR)[1] has yet to be solved in detail, although a low-resolution structure of the quaternary insulin−IR complex was reported recently (*1*). Therefore, insight into the mechanism of the insulin−IR interaction has so far been derived only from studies of the structures and activity of a variety of insulin mutants (*2*−*11*).

Insulin consists of two chains, a 21-residue A-chain and a 30-residue B-chain. In the native state insulin folds into a three-helical structure where the residues A2−A7, A13−A19, and B10−B19 form regular helices. The two helices in the A-chain are joined by a loop from A9 to A12 that brings the N- and C-termini together. The B-chain helix is followed by a turn and the C-terminal end of the B-chain is extended, making close nonbonding contacts to the B-chain helix. The N-terminal end of the B-chain is unstructured. When insulin monomers associate to dimers, the extended C-terminal ends of the two molecules are brought together, forming a two-stranded antiparallel β-sheet, which is stabilized by hydrophobic contacts and intermolecular hydrogen bonds.

Previous investigations of the superactive, monomeric des-[Phe(B25)]insulin mutant (*8*) showed that deletion of Phe(B25) caused Pro(B28) to move into the position normally occupied by Thr(B27). In consequence of this, the side chain of the proline residue is turned away from the dimer interface, thereby preventing the dimer-stabilizing hydrophobic contacts. This result suggests that moving Pro(B28) into position

[†] This work was financially supported by the Danish Natural Science Research Council (J 9400351 and J 9801801), Direktør Ib Henriksens Fond, Carlsbergfondet, and Novo Nordisk Fonden.

[‡] The ^{1}H chemical shifts of PT insulin in H_2O and in 35% TFE and the ^{13}C chemical shifts of PT insulin in 35% TFE have been deposited in the BioMagResBank (http://www.bmrb.wisc.edu), BMRB accession number 4997. NMR-derived restraints have been deposited in the RCSB (Research Collaboratory for Structural Bioinformatics) and the Protein Data Bank, accession numbers PDB 1JCO and RCSB RCSB013628, together with the coordinates of the 25 refined structures with lowest energy.

* Corresponding author: Telephone (+45) 3532 0302; fax (+45) 3535 0609; e-mail led@kiku.dk.

[§] University of Copenhagen.

[||] The Bartholin Institute.

[1] Abbreviations: DG, distance geometry; DQF-COSY, double quantum filtered correlation spectroscopy; FT, Fourier transformation; HSQC, heteronuclear single quantum correlation; IR, insulin receptor; NMR, nuclear magnetic resonance; NOE, nuclear Overhauser effect; NOESY, nuclear Overhauser effect spectroscopy; PT insulin, insulin analogue containing two substitutions in the B-chain [Thr(B27) → Pro and Pro(B28) → Thr]; SA, simulated annealing; TFE, 2,2,2-trifluoroethanol; TOCSY, total correlation spectroscopy; CSI, chemical shift index; HPLC, high-performance liquid chromatography; MALDI-TOF, matrix-assisted laser desorption ionization−time-of-flight; BSA, bovine serum albumin.

10.1021/bi0108150 CCC: $20.00
Published on Web 08/11/2001

B27 by interchanging Thr(B27) and Pro(B28) in native insulin would have the same effect and thus prevent aggregation. To investigate this hypothesis, we have carried out an NMR study of the structure and folding of the novel insulin analogue [Thr(B27) → Pro, Pro(B28) → Thr]insulin (PT insulin).

PT insulin is biologically active and can, therefore, assume the conformation necessary for its binding to the receptor. However, it is also unusually flexible and has a less well-defined structure in water. Therefore, to investigate its folding propensity, the structure and folding of the mutant were investigated both in pure water and in aqueous solution with different concentrations of trifluoroethanol (TFE). Thus, TFE strengthens helical structures in peptides and proteins and induces helical structures in segments that have the propensity of forming helices (*12, 13*). Trifluoroethanol has also been observed to stabilize β-turns and β-hairpins in proteins (*14, 15*). On the other hand, as a denaturant TFE disrupts the quaternary structure of proteins and reduces interactions between nonpolar residues (*16, 17*).

MATERIALS AND METHODS

Protein Synthesis, Purification, and Characterization. A pPIC9 plasmid containing cDNA encoding B[T(B27) → P,P-(B28) → T]-Lys-Arg-A miniproinsulin was inserted in *Pichia pastoris* and expressed during fermentation by methanol induction (*18*). PT insulin was obtained by sequential cleavage by trypsin and caboxypeptidase B and purified to homogeneity by preparative reverse-phase HPLC (*19*). The product was analyzed by MALDI-TOF and N-terminal amino sequencing, which both verified the correct product.

Activity of the Mutant. PT insulin was compared to human insulin by subcutaneous injection in 8−10 week old Balb-c mice. An amount of 0.001 unit (37 μg) of insulin per gram of mouse body weight was injected subcutaneously in the neck fold, and the blood glucose was measured in the tail vein at 10 min intervals for 60 min. The insulin was diluted in isotonic sodium chloride adjusted to pH 4.0 and containing 0.05% BSA (bovine serum albumin) to minimize surface adherence of insulin. The glucose-lowering effect of insulin was evaluated from the decrease of the blood glucose from 0 to 20 min and from 0 to 60 min after injection. PT insulin had a larger blood glucose-lowering effect than human insulin when injected in equimolar amounts (the integral above the glucose decay curve was 56.4 ± 10 for PT insulin vs 30.1 ± 4 for human insulin, $n = 6$, $P = 0.03$). When the injection of human insulin was repeated with a 50% increased dose, the blood glucose effect was similar to that for PT insulin (56.4 ± 10 vs 57.7 ± 9, $n = 6$, $P = 0.03$). In agreement with this, insulin receptor binding studies showed that PT insulin has binding characteristics similar to those of human insulin ($K_d = 5.2 \times 10^{-12}$ M for PT insulin vs $K_d = 3.6 \times 10^{-12}$ M for human insulin). A detailed description of the synthesis, purification, characterization, and activity of PT insulin will be published elsewhere.

NMR Spectroscopy. Samples of the mutant in water and TFE/water solution were prepared by dissolving the lyophilized protein in 90%/10% H_2O/D_2O with the appropriate amount of 2,2,2-trifluoroethanol-d_3 to a protein concentration of 2.8 mM. The pH was adjusted to 3.13−3.21 by addition of HCl. The samples were stored at 5 °C between experiments. All NMR experiments were carried out at 25 °C, except the amide proton exchange experiments, which were done at 15 °C. Two-dimensional NMR spectra, DQF-COSY (*20*), ^{1}H−^{1}H TOCSY (*21*), ^{1}H−^{1}H NOESY (*22*), and ^{1}H−^{13}C HSQC (*23*) were recorded on 500 and 800 MHz Varian Unity Inova spectrometers. The WaterGate pulse sequence (*24*) was used for solvent suppression in the NOESY and TOCSY spectra. The TOCSY spectra were recorded with mixing times of 30, 60, and 90 ms, while the NOESY spectra were recorded with mixing times of 120 and 180 ms. In the spectra recorded at 500 and 800 MHz the ^{1}H spectral widths were 8000 and 10 000 Hz, respectively. The number of data points in the t_2 dimension was 4096 in all cases, while the number of increments in the t_1 dimension was between 300 and 512, except for the amide proton exchange experiments, where 60 t_1 increments were used. The spectra were recorded in the phase-sensitive mode by use of the States−Haberkorn−Ruben scheme (*25*). The HSQC spectra were obtained with ^{13}C spectral widths of 18 752 and 30 007 Hz at 125 and 200 MHz, respectively, and 512 t_1 increments. The ^{1}H−^{13}C HSQC spectra were acquired with ^{13}C in natural abundance.

Fourier transformation and processing of the spectra were performed with the program NMRPipe (*26*), while spectral assignments were carried out with the program XEASY (*27*). Chemical shifts were measured in parts per million relative to water (4.774 ppm at 25 °C; *28*). Examples of one- and two-dimensional spectra of PT insulin in H_2O and 35% TFE are shown in Figure 1.

TFE Titration. Six 800 MHz ^{1}H-NOESY spectra of PT insulin dissolved in water with different concentrations of TFE were recorded at 25 °C and pH 3.02 (meter reading). The TFE concentration was varied from 0% to 25% by successive addition of aliquots of 40 μL of TFE. Accordingly, the insulin concentration was varied from 3.1 to 2.3 mM.

Amide Proton Exchange Experiments. A ^{1}H−^{1}H NOESY spectrum of PT insulin recorded at 25 °C and pH 3.21 immediately after dissolution in D_2O did not contain any amide proton resonances, which shows that the NH exchange rate of the amide protons in water is high. To obtain a quantitative measure of the NH exchange rates, a series of six consecutive NOESY spectra were recorded by the following procedure. At 15 °C a total of 10 mg of PT insulin was dissolved in a minimum amount of water (200 μL), and pH was adjusted to 3.00 (meter reading) by addition of DCl. At $t = 0$ a total of 400 μL of D_2O (15 °C, pD = 3.00) was added, and immediately thereafter the sample was placed in the spectrometer at 15 °C and the experiment was started. The time from the dissolution to the start of the experiment was less than 10 min. The spectra were recorded with 96 transients in order to gain a high signal-to-noise ratio. A total of 4096 data points were used in the t_2 dimension, while 60 increments were used in the t_1 dimension. The total recording time was 6 h for each of the six spectra. Since the spectra contained residual signals from all the amide protons, the slow-exchanging amide protons were identified from difference spectra. These spectra were generated by subtracting the last spectrum recorded (number six containing the weakest signals) from each of the preceding five spectra prior to Fourier transformation.

A slightly different procedure was applied in the exchange experiment in TFE/water because of the much slower exchange rates of the amide protons in this solvent. Thus,

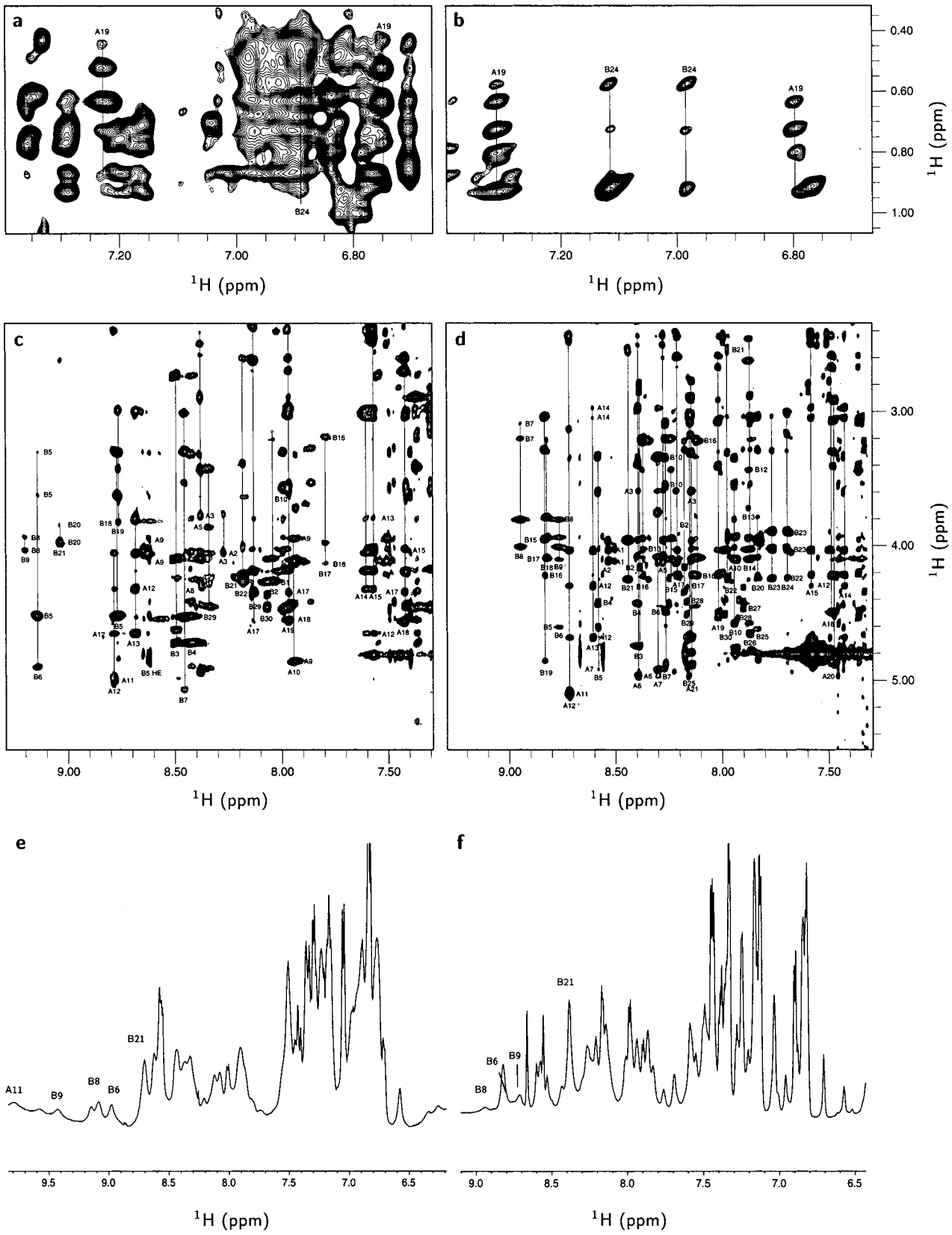

FIGURE 1: Amide/aromatic region of ^{1}H−^{1}H NOESY spectra of PT insulin. Upper panels show the region correlating aromatic side-chain protons and aliphatic side-chain protons in (a) pure water and (b) 35% TFE. Middle panels show the fingerprint area of the NOESY spectra of PT insulin in (c) H_2O and (d) 35% TFE-d_3. Notice that the spectrum in TFE has more sequential NOEs and sharper signals. Lower panels show the amide/aromatic region of the 1D spectra of PT insulin in (e) H_2O and (f) 35% TFE-d_3.

immediately before the experiment was started, 11 mg of PT insulin was dissolved in 550 μL of 35% TFE/65% D_2O and the pH was adjusted to 3.04 (meter reading) with perdeuterated acetic acid. The total time from the dissolution of the protein to the start of the experiment was less than 10 min. The exchange experiment in TFE was carried out at

15 °C, with the same spectral parameters as in the experiment in pure H_2O/D_2O in order to allow a direct comparison of the exchange rates in the two solvents.

Measurement of NH Exchange Rate Constants. The intensities I of the cross-peaks were calculated by a procedure provided with the XEASY package and based on the integration approach proposed by Denk et al. (*29*). The intensities obtained from the spectra of the mutant in 35% TFE were subsequently fitted to the single-exponential function, $I = I_0 \exp(-k_{obs}t)$, where k_{obs} is the exchange rate constant, and I_0 is the intensity at $t = 0$. The intensities obtained from the spectra of the mutant in 67% D_2O/33% H_2O were fitted to the exponential function $I = {}^1/_3 I_0[1 + 2 \exp(-k_{obs}t)]$, to account for the fraction of H_2O and the reverse NH exchange ($^1H \rightarrow D$).

Protection Factors. Intrinsic exchange rates for the slow-exchanging amide protons were determined by the method of Bai et al. (*30*). The protection factors were defined as $P = k_{int}/k_{obs}$, where k_{int} is the intrinsic exchange rate constant and k_{obs} is the experimentally derived exchange rate constant.

Structure Calculation. Interproton distances were obtained from $^1H-^1H$ NOESY spectra recorded with a mixing time of 120 ms. The intensities of the cross-peaks were obtained with XEASY (see above) and classified as strong, medium, and weak with upper-bound distances of 2.80, 3.50, and 5.00 Å, respectively. For each hydrogen bond two distance restraints were used, i.e., one (1.8−2.0 Å) for the O−H distance and one (1.8−3.0 Å) for the O−N distance. Torsion angles were obtained from the program TALOS (*31*) by use of $^1H^\alpha$, $^{13}C^\alpha$, and $^{13}C^\beta$ secondary chemical shifts.

The structures were calculated with X-PLOR 3.851 (*32*). First, distance geometry (DG) substructures were calculated with the Metric Matrix algorithm (*33*) and the protocol DG-SUB-EMBED. Second, simulated annealing was applied with the DGSA protocol. The structures were initially run through 200 steps of restrained Powell energy minimization. Subsequently, 3 ps restrained molecular Verlet dynamics (RMD) calculations were performed at 3000 K, followed by 3 ps cooling to 300 K. The temperature was varied in steps of 50 K during cooling, and RMD was performed after each temperature step. All structures were subsequently subjected to 1200 steps of restrained energy minimization. Finally the structures were refined with the simulated annealing REFINE protocol. Simulated annealing (as described above) was again followed by 1200 steps of restrained energy minimization. The van der Waals energy function was represented by a simple repel function. During the cooling stage the force constant of the van der Waals repel function was varied from 0.003 to 4 kcal mol^{-1} $Å^{-4}$. The force constants on the NOE and dihedral angle restraints were 50 kcal mol^{-1} $Å^{-2}$ and 200 kcal mol^{-1} rad^{-2}, respectively. The three disulfide bridges were treated as covalent bonds in the calculations.

RESULTS

Sequential Assignments. Complete sequential assignments of the ^1H and ^{13}C resonances of PT insulin in 35% TFE were achieved by well-established procedures on the basis of the 2D TOCSY, NOESY, and $^1H-^{13}C$ correlated HSQC spectra. The spectra of PT insulin in pure water could only be partly assigned due to missing sequential correlations and broad resonance lines, as explained below. The assigned chemical shifts are given as Supporting Information and also have been deposited in the BioMagResBank (http://www.bmrb.wisc.edu), BMRB accession number 4997.

PT Insulin in H_2O versus TFE/H_2O. The NMR spectra of the biologically active PT insulin dissolved in H_2O are characterized by a large chemical shift dispersion, which suggests that the tertiary insulin fold is conserved. Thus, as in other biologically active insulin mutants, the signal from Cys(A11)-NH is observed at extreme low field (9.79 ppm), while the signals of the NH protons of Leu(B6), Gly(B8), Ser(B9), and Glu(B21) are found in the region 8.9−9.5 ppm (see Figure 1c,e). Similarly, signals from the aliphatic side-chain protons of Leu(B15) are located at very high field (0.02−0.4 ppm). On the other hand, relatively few sequential and medium-range NOEs are observed while all amide protons are fast-exchanging at 25 °C. Immediately these observations suggest a relatively loose secondary structure of the mutant. Furthermore, the NMR signals of PT insulin in water are relatively broad and increase in line width with increasing temperature and magnetic field strength, in some cases even beyond recognition. These observations indicate that PT insulin is present in more than one conformation and that the line broadening is due to exchange between different conformations. The latter could also reflect a weak association of monomers, although this possibility seems less important than exchange between different conformations considering its temperature and field dependences and the lack of slowly exchanging amide protons and sequential and medium-range NOEs. The line broadening and the small number of sequential correlations (see Figure 1c,e) have so far prevented a complete sequential assignment of the spectra of PT insulin in H_2O.

In water with 35% TFE, the signals of PT insulin become significantly sharper, as shown in Figure 1b,d,f. Furthermore, numerous sequential and medium-range NOEs appear while 12 slowly exchanging amide protons are observed in D_2O at 15 °C. These observations are consistent with the formation of well-defined secondary structure elements. On the other hand, fewer long-range NOEs are observed in 35% TFE and the dispersion of the signals is significantly reduced. This is consistent with the ability of TFE to disrupt tertiary structure.

Amide Proton Exchange and Hydrogen Bonds. More detailed information about the structure of PT insulin in pure water was obtained from the exchange of the amide protons at lower temperature. Thus, while amide protons of PT insulin were exchanging too fast in D_2O/H_2O at 25 °C to be observed, a few of the amide protons showed NOESY cross-peaks at 15 °C that were sufficiently intense to allow their exchange rates to be measured by the approach described under Materials and Methods. Figure 2a shows the first spectrum in the amide proton exchange experiment of PT insulin recorded after 6 h in 67% D_2O/33% H_2O, while Figure 2b shows the difference spectrum between the last spectrum recorded in this series (after 36 h in 67% D_2O/33% H_2O) and the spectrum in Figure 2a. The exchange rates and the corresponding protection factors (*30*) are listed in Table 1. As it appears from Table 1, the protection factors are very small. The minimum strength of a regular hydrogen bond is approximately 8 kJ mol^{-1} (*34*), corresponding to a protection factor $P_{min} \approx 26$ at 15 °C. Therefore, the protection factors obtained here suggest that the slowly exchanging

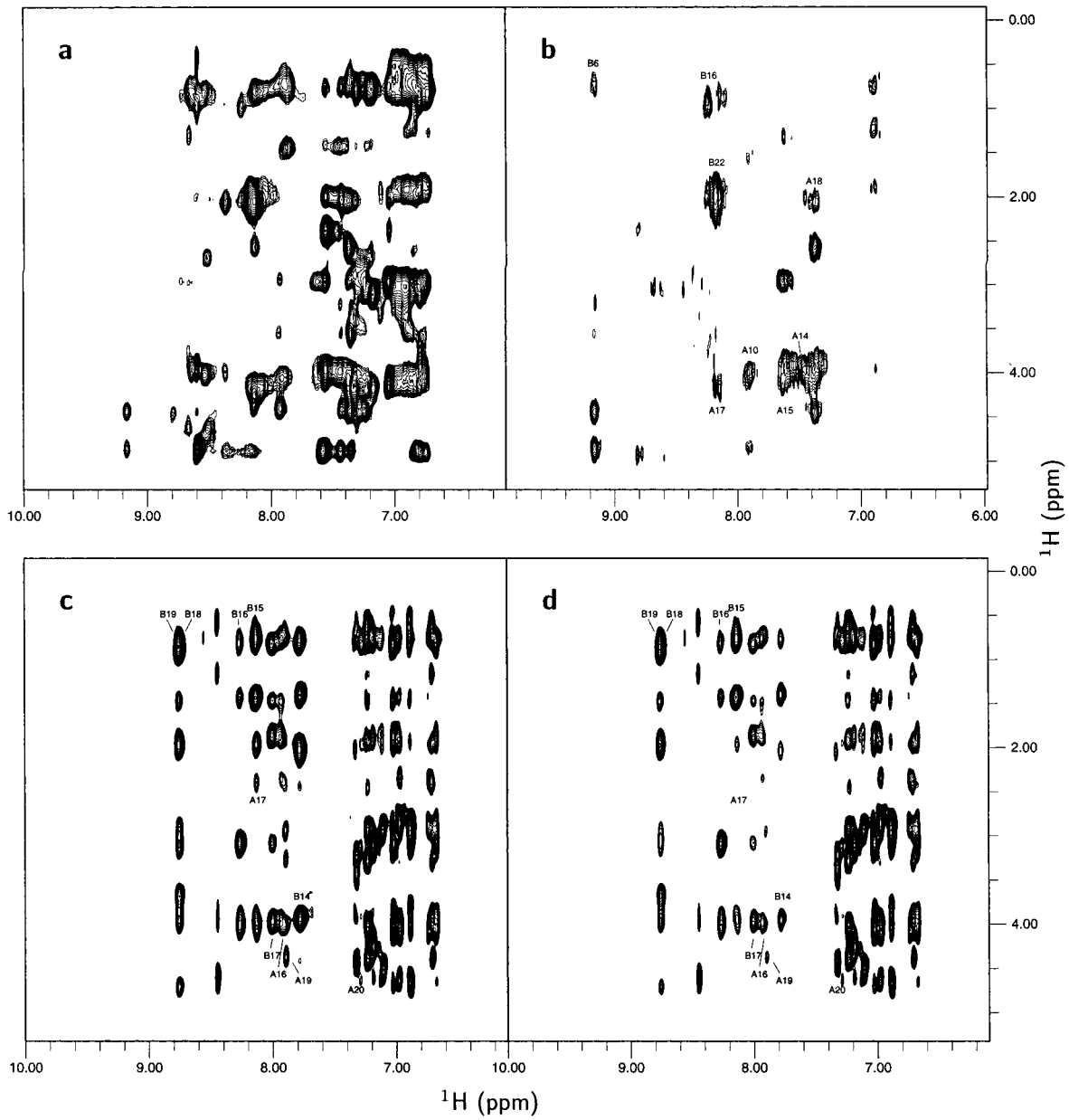

FIGURE 2: Amide/aromatic region of ^{1}H−^{1}H NOESY spectra of PT insulin in pure water (upper panels) and in 35% TFE/65% D_2O (lower panels): (a) first NOESY spectrum of PT insulin in 33% H_2O/67% D_2O, recorded during the first 6 h after dissolution in 33% H_2O/67% D_2O; (b) difference spectrum between the spectrum in panel a and the spectrum of the sample recorded after 36 h; (c) first NOESY spectrum of PT insulin in 35% TFE/65% D_2O, recorded during the first 6 h after dissolution in D_2O; (d) after 36 h in D_2O. A substantial amount of amide protons are slowly exchanging, as shown by the presence of the amide proton signals after 36 h in D_2O.

amide protons of PT insulin in pure water are only weakly hydrogen-bonded.

Four of the slowly exchanging amide protons in PT insulin are found in the native helical regions, that is, Tyr(A14), Gln(A15), Glu(A17), and Tyr(B16). The first three of these indicate that part of the C-terminal A-helix (A_{II}-helix) is loosely established in water. Indeed this is supported by the $^{13}C^{\alpha}$ chemical shift indices (CSIs) in H_2O (see below and Figure 6). The slow exchange of the Tyr(B16)-NH and the $^{13}C^{\alpha}$ CSIs of the residues of the central part of the B-chain (Figure 2) indicate that the B-chain helix also is established, although it is even looser than the A_{II}-helix.

The slow exchanges of the Leu(B6) and Arg(B22) amide protons suggest that also part of the tertiary structure of native insulin is loosely established in PT insulin in pure water. Thus, in the crystallographic T-state of native insulin, Leu(B6)-NH forms an interchain hydrogen bond to the backbone carbonyl oxygen of Cys(A6), while Arg(B22) is hydrogen-bonded to the carbonyl oxygen of Cys(B19) (*35*). Therefore, these hydrogen bonds are associated with the tertiary structure; the former defines the relative orientation of the two N-termini, while the latter stabilizes the turn following the B-chain helix. The remaining slowly exchanging amide proton in PT insulin, that is, Ile(A10)-NH, corresponds to a very weak hydrogen bond according to the exchange rate and the protection factor (Table 1). A similar slow exchange has not been reported for this amide proton in any other insulin monomer.

For PT insulin dissolved in 65% D_2O/35% TFE, significantly slower amide proton exchange rates were observed. Figure 2c,d show spectra recorded 6 and 36 h after dissolution, respectively. After 36 h a substantial amount of

Table 1: Exchange Rates and Protection Factors for PT Insulin in H_2O and in 35% TFE

	in 35% TFE/65% D_2O			in pure D_2O		
residue	k_{obs} (h^{-1})	k_{int} (h^{-1})	P	k_{obs} (h^{-1})	k_{int} (h^{-1})	P
IleA10				0.258 ± 0.029	0.554	2.1
TyrA14				0.185 ± 0.004	0.894	4.8
GlnA15	0.00570 ± 0.0012	1.872	328	0.100 ± 0.009	1.872	18.7
LeuA16	0.0121 ± 0.0002	0.766	62			
GluA17	0.0403 ± 0.0011	1.978	49	0.444 ± 0.145	1.978	4.4
TyrA19	0.0201 ± 0.0006	1.897	94			
CysA20	0.105 ± 0.008	5.178	49			
LeuB6				0.233 ± 0.021	1.978	10.27
AlaB14	0.0228 ± 0.0004	3.997	174			
LeuB15	0.00629 ± 0.0005	0.776	123			
TyrB16	0.00733 ± 0.0002	0.894	121	0.444 ± 0.111	0.894	2.0
LeuB17	0.0124 ± 0.0004	0.572	46			
ValB18	0.0116 ± 0.0002	0.377	32			
CysB19	0.0148 ± 0.0007	3.411	230			
ArgB22				0.582 ± 0.211	3.971	6.81

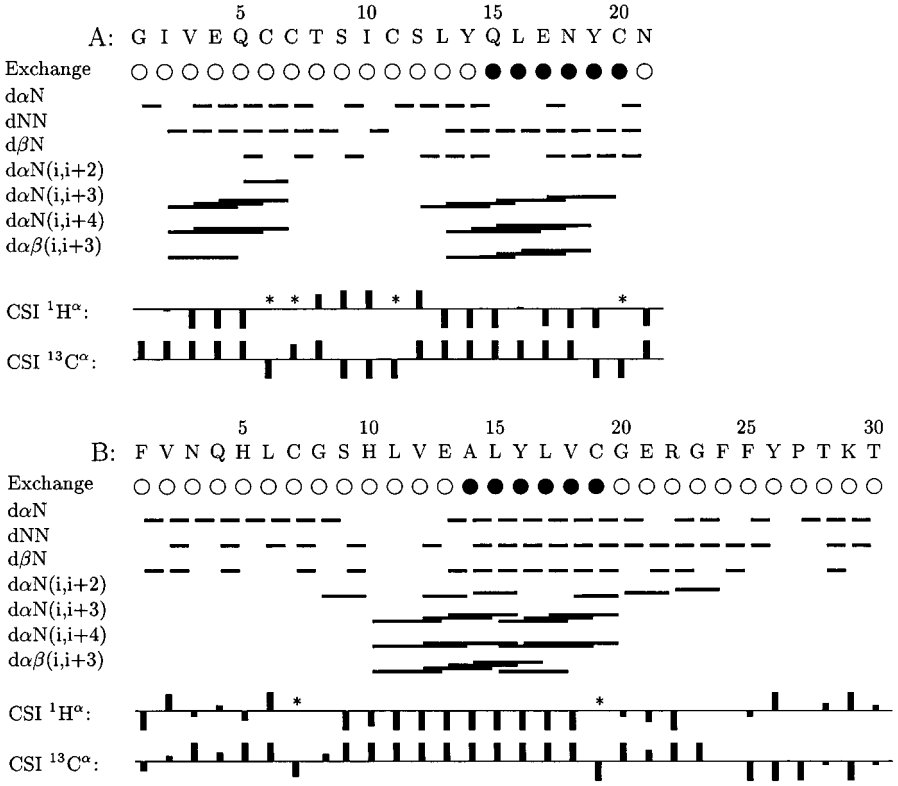

FIGURE 3: Sequential and medium-range NOE connectivities and $^1H^\alpha$ and $^{13}C^\alpha$ chemical shift indices of PT insulin in 35% TFE. Slow- and fast-exchanging backbone amide protons are indicated by filled (●) and empty (○) circles, respectively. The chemical shift indices (CSIs) were calculated as the difference between the experimental chemical shifts and the random coil values (*28*). For the glycine residues, the chemical shift indices were calculated from the average chemical shift of the two α-protons. No $^1H^\alpha$ chemical shift indices are given for the six disulfide-bonded cysteine residues, as indicated by asterisks.

amide protons is still present. The exchange rates of the slowly exchanging amide protons and the corresponding protection factors are given in Table 1. All of the slowly exchanging amide protons are from residues in the helical regions. The magnitudes of the exchange rate constants and protections factors clearly indicate that they are all engaged in regular hydrogen bonds.

Structure of PT Insulin in TFE. The sequential and medium-range NOEs found for PT insulin in the presence of 35% TFE are summarized in Figure 3, together with the slowly exchanging amide protons and the $^1H^\alpha$ and $^{13}C^\alpha$ CSIs. The pattern of $d\alpha N(i, i + 3)$, $d\alpha N(i, i + 4)$, and $d\alpha\beta(i, i + 3)$ connectivities establishes that the A-chain contains two α-helices (A_I, residues A2−A7, and A_{II}, residues A13−A19; upper panel in Figure 3), while the B-chain contains a central α-helix (residues B10−B20, lower panel in Figure 3). These helices correspond closely to those found in native insulin. The presence of the A_{II}- and B-helices is confirmed by the slowly exchanging amide protons in D_2O (Figure 3) and by consecutive stretches of negative $^1H^\alpha$ and positive $^{13}C^\alpha$ CSIs. The absence of slowly exchanging amide protons in the N-terminal segment of the A-chain indicates that the A_I-helix is less well-defined than the A_{II}- and B-helices.

A limited number of long-range NOEs are also observed in the NOESY spectra of PT insulin dissolved in TFE, but most of the long-range contacts found for insulins with the native fold are absent. This is consistent with a disruption of hydrophobic contacts. However, long-range contacts are found between Ile(A2) $^1H^\gamma/^1H^\delta$ and Tyr(A19) $^1H^\delta/^1H^\epsilon$, indicating that the two A-chain termini are brought together

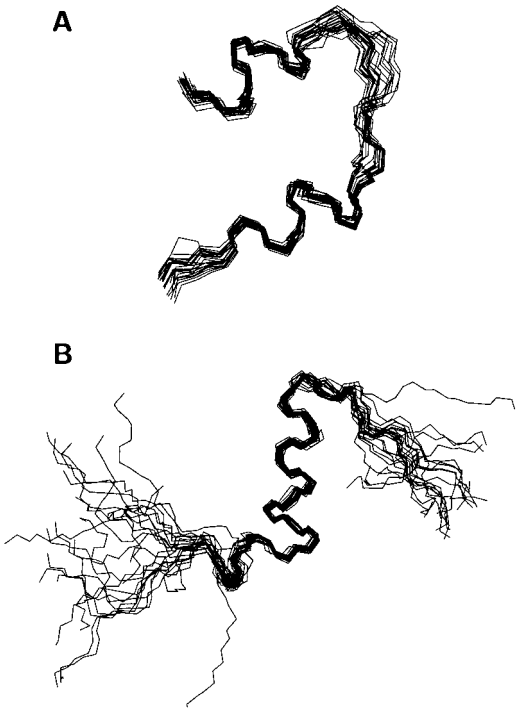

FIGURE 4: Superposition of the 24 structures of PT insulin with the lowest total energy: (A) the A-chain and (B) the B-chain.

as in native insulin. Other long-range contacts are observed between Leu(B15) $^1H^\delta$ and Phe(B24) $^1H^\delta/^1H^\epsilon$ and between Asn(A21) $^1H^\beta$ and Phe(B24) $^1H^\delta/^1H^\epsilon$. However, NOEs between the N-terminal A-chain and the C-terminal B-chain, as observed in native insulin, are absent in PT insulin in the presence of TFE. Also, the signals from the four N-terminal residues in the B-chain are among the sharpest signals in the spectra. These observations show that the N-terminus of the B-chain is detached from the rest of the molecule and highly mobile. Figure 4 shows a superposition of the 24 structures with the lowest total energy. The structures were calculated from 197 distance restraints, 26 ϕ and 26 ψ dihedral angle restraints, and 11 hydrogen bonds, by the procedure described under Materials and Methods. The total number of restraints and the structural statistics are summarized in Table 2.

TFE Titration. The large difference between the spectra of PT insulin in 35% TFE and pure water prompted a detailed investigation of the differences by following the spectral changes as a function of the TFE concentration. Unfortunately, this approach was hampered by a large variation in the appearance and complexity of the proton spectra, especially at the lower TFE concentrations as shown in Figure 5, which prevents an assignment of the spectra in pure water by this approach. However, the titration series reveals that the $^{13}C^\alpha$ chemical shifts remain almost constant throughout the titration series, with positive CSIs in the regions of the native helices, as seen in Figure 6. Despite the fact that only part of the $C^\alpha-H^\alpha$ correlations appear at low TFE concentrations and in pure water, due to the line broadening caused by conformational exchange (see above), these results on the C^α chemical shifts suggest that precursors of the helices are formed in pure water, although only rather loosely as indicated by the fast amide proton exchanges.

Table 2: Structural Statistics of PT Insulin in 35% TFE

Number of Constraints	
total number of NOEs	197
intraresidual NOEs	33
sequential NOEs [$d_{i,j}$, $(j - i) \leq 5$]	128
long-range NOEs	36
dihedral angles	52
hydrogen bonds	11
Rmsd from NOE Restraints and from the Idealized Geometry Used within X-PLOR	
NOE (Å)	0.042 (± 0.006)
dihedral angles (deg)	0.83 (± 0.08)
bond length (Å)	0.0023 (± 0.0002)
bond angles (deg)	0.44 (± 0.01)
improper dihedral angles (deg)	0.32 (± 0.02)
PROCHECK (*36*) Ramachandran Analysis	
most favored regions (%)	70.9
additional allowed regions (%)	17.4
generously allowed regions (%)	9.1
disallowed regions (%)	2.6
Average Rmsd of the Final Ensemble	
backbone atoms (A2 → A7) (Å)	0.16
backbone atoms (A13 → A19) (Å)	0.15
backbone atoms (B10 → B19) (Å)	0.16
all backbone atoms (Å)	4.62
all heavy atoms (Å)	5.65

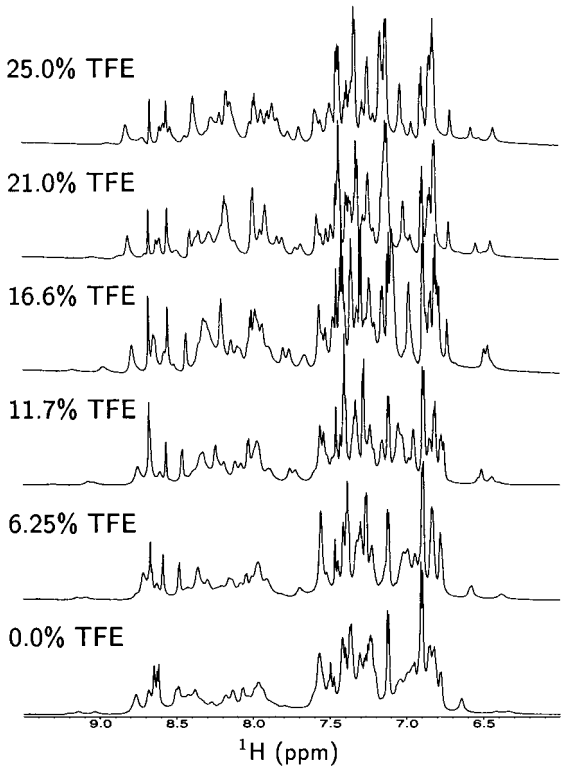

FIGURE 5: One-dimensional ^{1}H spectra of the amide/aromatic region of PT insulin showing the variation in the number of signals, chemical shifts, and line widths as a function of the TFE concentrations. The intensities of signals in different spectra are not comparable due to different scaling.

DISCUSSION

Structure of PT Insulin in Pure Water. The results obtained here clearly show that even though PT insulin is very flexible in H_2O and assumes more conformations, it has the propensity to form the native secondary fold. This is revealed both by the folding of the mutant when exposed to TFE and by the helical precursor in pure water indicated by the $^{13}C^\alpha$ CSIs (Figure 6) and the amide proton exchange rate (Table 1).

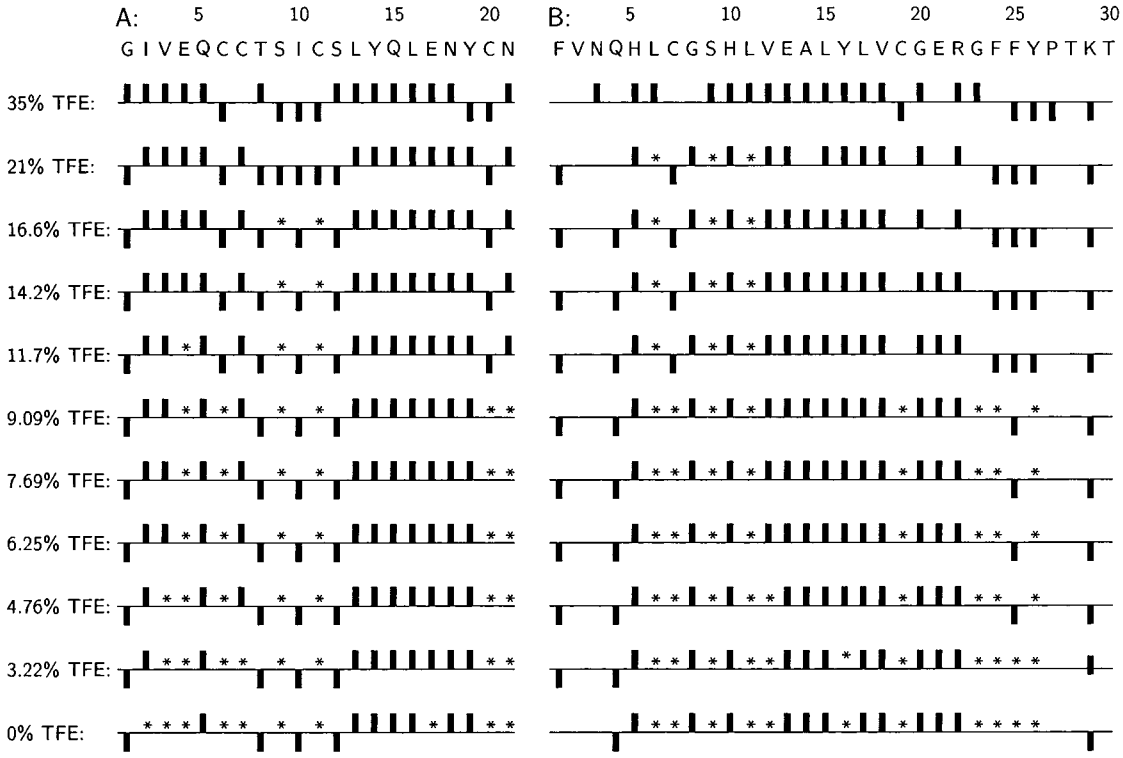

FIGURE 6: Chemical shift indices of $^{13}C^{\alpha}$ in PT insulin obtained from the HSQC spectra in the TFE titration series. Asterisks indicate residues for which no $^{13}C^{\alpha}-H^{\alpha}$ correlation was observed.

However, the absence of genuine hydrogen bonds associated with the secondary structure and the lack of sequential and medium-range NOEs suggest that the secondary structure is very loose in pure water.

Furthermore, several features of the spectra of PT insulin in H_2O indicate that the mutant assumes a tertiary structure similar to that of native insulin, despite its high flexibility. These features are (1) the large dispersion of the resonances, including the extreme chemical shift values of a series of residues [0.02−0.4 ppm for the side-chain protons of Leu(B15) and 9.79, 9.43, 9.15, and 9.08 ppm for the amide protons of Cys(A11), Gly(B8), Ser(B9), and Leu(B6), respectively] that in other insulins are associated with the tertiary structure; (2) the large amount of tertiary contacts [between Tyr(A14) and Ile(A10), Tyr(A19) and Ile(A2)/Val(A3)/Leu(B15), Phe(B25) and Leu(B15)/Val(B12), His(B5) and Ile(A10), and Tyr(B26) and Leu(B15)/Ile(A2), as well as numerous unassigned correlations between aromatic and aliphatic side-chain protons]; (3) the $^{13}C^{\alpha}$ chemical shift indices; and (4) the slow exchange rates of the amide protons of Leu(B6) and Arg(B22), which in the native fold of insulin are hydrogen-bonded to the carbonyl groups of Glu(A4) and Val(B19), respectively. All taken together, these findings imply that the solution conformation of PT insulin corresponds to the overall globular structure of native insulin but with a poorly defined secondary structure.

Implications for Receptor Binding. It is well-established that flexibility is crucial for the function of insulin (*2, 3, 10*), indicating that transient structural changes are required for the binding of insulin to its receptor. It is, therefore, obvious to associate the increased biological activity of PT insulin with its high flexibility. Furthermore, the lack of a genuine secondary structure in PT insulin dissolved in water shows that secondary structure is unnecessary for the biological activity of free insulin. Only the propensity to form the native secondary structure upon binding to the receptor, and a flexible globular structure as found here for PT insulin in water, seem to be required.

More specifically, this conclusion should be compared with previous results which show that the N-terminal A_I-helix is important in receptor interaction (*7, 9, 11*), and that the activity of insulin is related to the helix-forming propensity of the amino acids of the A_I-helix (*11*). The results obtained here not only support these findings but also suggest that the presence of the A_I-helix in the free insulin molecule is not essential to receptor binding; only the propensity to form the helix upon binding to the receptor is required. In fact, the increased activity of PT insulin as compared to native insulin suggests that an unstructured or loosely structured form of the molecule, including the N-terminal end of the A-chain, favors the receptor binding. Thus, the loose structure of PT insulin and its high flexibility may facilitate the binding process, i.e., increase the association rate, while the propensity of PT insulin to form the structure of native insulin ensures a correct binding to the receptor. This may indicate that the association rate rather than the equilibrium binding is the important factor for the biological action. Furthermore, it leads to the suggestion that in native insulin, where the A_I-helix is well-established in the free molecule in solution, a partial unfolding of this helix is necessary prior to the receptor binding in order for the insulin molecule to navigate into the receptor binding site. Subsequently, the A_I-helix refolds to accommodate the binding site, ensuring a tight insulin−receptor binding. Thus, the initial unfolding of the A_I-helix in native insulin during the binding process may explain its lower activity as compared to PT insulin.

In conclusion, we suggest a mechanism for the insulin receptor binding as shown schematically in Figure 7. The

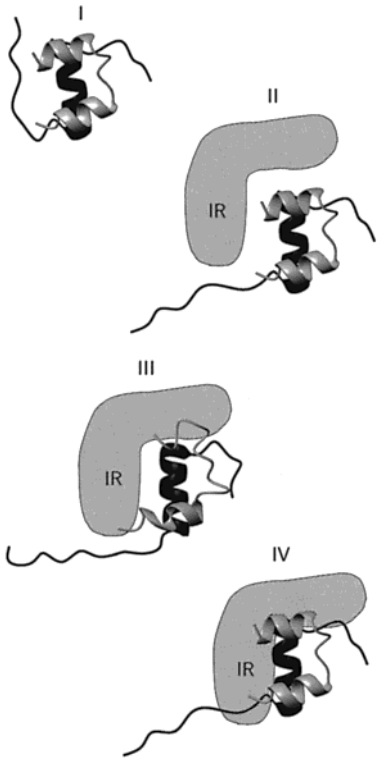

FIGURE 7: Model of the insulin−receptor interaction. I, free insulin in solution; II, detachment of the C-terminal part of the B-chain from the rest of the molecule; III, unfolding of the A_I-helix; IV, refolding of A_I-helix after navigation into the binding site of the receptor. The A-chain is shown in light gray, the B-chain is shown in black, and the insulin receptor is represented schematically by a gray object.

mechanism also includes a detachment of the C-terminal end of the B-chain from the rest of the molecule before receptor interaction can take place, as found in previous studies (*2*, *3*, *10*).

ACKNOWLEDGMENT

The 750 and 800 MHz NOESY and HSQC spectra were obtained at The Danish Instrument Centre for NMR Spectroscopy of Biological Macromolecules. We are grateful to Ms. Else Philipp and Dr. Jens Duus for technical assistance. D.K. acknowledges a travel scholarship to the Keystone meeting, January 2001, from Acta Chemica Scandinavica, The Danish Chemical Society.

SUPPORTING INFORMATION AVAILABLE

Tables of chemical shifts: the ^1H chemical shifts of PT insulin in H_2O and in 35% TFE, and the ^{13}C chemical shifts of PT insulin in 35% TFE (PDF). This material is available free of charge via Internet at http://pubs.acs.org.

REFERENCES

1. Luo, R. Z. T., Beniac, D. R., Fernandez, A., Yip, C. C., and Ottensmeyer, F. P. (1999) *Science 285*, 1077−1080.
2. Derewenda, U., Derewenda, Z., Dodson, E. J., Dodson, G. G., Bing, X., and Markussen, J. (1991) *J. Mol. Biol. 220*, 425−433.
3. Hua, Q. X., Shoelson, S. E., Kochoyan, M., and Weiss, M. A. (1991) *Nature 354*, 238−241.
4. Nakagawa, S. H., and Tager, H. S. (1992) *Biochemistry 31*, 3204−3214.
5. Hua, Q. X., Kochoyan, M., and Weiss, M. A. (1992) *Proc. Natl. Acad. Sci. U.S.A. 89*, 2379−2383.
6. Ludvigsen, S., Roy, M., Thøgersen, H., and Kaarsholm, N. C. (1994) *Biochemistry 33*, 7998−8006.
7. Hua, Q. X., Hu, S. Q., Frank, B. H., Jia, W., Chu, Y. Q., Wang, S. H., Burke, G. T., Katsoyannis, P. G., and Weiss, M. A. (1996) *J. Mol. Biol. 264*, 390−403.
8. Jørgensen, A. M. M., Olsen, H. B., Bahlschmidt, P., and Led, J. J. (1996) *J. Mol. Biol. 257*, 684−699.
9. Olsen, H. B., Ludvigsen, S., and Kaarsholm, N. C. (1998) *J. Mol. Biol. 284*, 477−488.
10. Ludvigsen, S., Olsen, H. B., and Kaarsholm, N. C. (1998) *J. Mol. Biol. 279*, 1−7.
11. Weiss, M. A., Hua, Q. X., Jia, W., Chu, Y. C., Wang, R. Y., and Katsoyannis, P. G. (2000) *Biochemistry 39*, 15429−15440.
12. Buck, M., Radford, S. E., and Dobson, C. S. (1993) *Biochemistry 32*, 669−678.
13. Hamada, D., Kuroda, Y., Tanaka, T., and Goto, Y. (1995) *J. Mol. Biol. 254*, 737−746.
14. Blanco, F. J., Ortiz, A. R., and Serrano, L. (1994) *Folding Des. 2*, 123−133.
15. Mabrouk, K., van Rietschoten, J., Rochat, H., and Loret, E. P. (1995) *Biochemistry 34*, 8294−8298.
16. Albert, J. S., and Hamilton, A. D. (1995) *Biochemistry 34*, 984−990.
17. Buck, M. (1998) *Q. Rev. Biophys. 31*, 297−355.
18. Invitrogen product manual, Pichia Expression Kit, Invitrogen Corporation.
19. Thim, L., Hansen, M. T., Norris, K., Hoegh, I., Boel, E., Forstrom, J., Ammerer, G., and Fiil, N. P. (1986) *Proc. Natl. Acad. Sci. U.S.A. 83*, 6766−6770.
20. Piantini, U., Sørensen, O. W., and Ernst, R. R. (1982) *J. Am. Chem. Soc. 104*, 6800−6801.
21. Braunschweiler, L., and Ernst, R. R. (1983) *J. Magn. Reson. 53*, 521−528.
22. Jeener, M., Meier, B. H., Bachman, P., and Ernst, R. R. (1979) *J. Chem. Phys. 71*, 4546−4553.
23. Bodenhausen, G., and Reuben, D. J. (1980) *J. Chem. Phys. 69*, 185−189.
24. Piotto, M., Saudek, V., and Sklenář, V. (1992) *J. Biomol. NMR 2*, 661−665.
25. States, D. J., Haberkorn, R. A., and Ruben, D. J. (1982) *J. Magn. Reson. 48*, 286−292.
26. Delaglio, F., Grzesiek, S., Vuister, G. W., Zhu, G., Pfeifer, J., and Bax, A. (1995) *J. Biomol. NMR 6*, 277−293.
27. Bartels, C., Xia, T., Billeter, M., Güntert, P., and Wüthrich, K. (1995) *J. Biomol. NMR 5*, 1−10.
28. Wishart, D. S., and Sykes, B. D. (1994) *Methods Enzymol. 239*, 363−340.
29. Denk, W., Baumann, R., and Wagner, G. (1986) *J. Magn. Reson. 67*, 386-390.
30. Bai, Y., Milne, J. S., Mayne, L., and Englander, W. (1993) *Proteins: Struct., Funct., Genet. 17*, 75−86.
31. Cornilescu, G., Delaglio, F., and Bax, A. (1999) *J. Biomol. NMR 13*, 289−302.
32. Brünger, A. T. (1992) in *X-PLOR manual*, Yale University Press, New Haven, CT.
33. Crippen, G. M., and Havel, T. F. (1988) *Distance Geometry and Molecular Conformation*, Research Studies Press Ltd., Taunton, Somerset, U.K.
34. Creighton, T. E. (1993) in *Proteins. Structure and Molecular Properties*, W. H. Freeman and Company, New York.
35. Baker, E. N., Blundell, T. L., Cutfield, J. F., Cutfield, S. M., Dodson, E. J., Dodson, G. G., Hodgkin, D. M. C., Hubbard, R. E., Isaacs, N. W., Reynolds, C. D., Sakabe, K., Sakabe, N., and Vijayan, N. M. (1988) *Philos. Trans. R. Soc. London, Ser. B 319*, 369−456.
36. Laskowski, R. A., Rullmann, J. A. C., MacArthur, M. W., Kaptein, R., and Thornton, J. M. (1996) *J. Biomol. NMR 8*, 477−485.

BI0108150